

Aeidapu MAHESH, Kanwarjit Singh SANDHU

A genetic algorithm based improved optimal sizing strategy for solar-wind-battery hybrid system using energy filter algorithm

© Higher Education Press and Springer-Verlag Berlin Heidelberg 2017

Abstract In this paper, the genetic algorithm (GA) is applied to optimize a grid connected solar photovoltaic (PV)-wind-battery hybrid system using a novel energy filter algorithm. The main objective of this paper is to minimize the total cost of the hybrid system, while maintaining its reliability. Along with the reliability constraint, some of the important parameters, such as full utilization of complementary nature of PV and wind systems, fluctuations of power injected into the grid and the battery's state of charge (SOC), have also been considered for the effective sizing of the hybrid system. A novel energy filter algorithm for smoothing the power injected into the grid has been proposed. To validate the proposed method, a detailed case study has been conducted. The results of the case study for different cases, with and without employing the energy filter algorithm, have been presented to demonstrate the effectiveness of the proposed sizing strategy.

Keywords PV-wind-battery hybrid system, size optimization, genetic algorithm

1 Introduction

The day-to-day increasing load demand and the global environmental pollution crisis have been raising the concerns worldwide for alternative, clean and sustainable energy sources. The renewable energy sources, which are abundantly available in nature, surely have the potential to solve the present energy crisis. Wind energy is one of the clean and promising sources and can easily be extracted by

means of wind turbines. And solar photovoltaic (PV) energy is the other source, which has a great potential as it is available around the globe. But, the only problem with these sources is their unpredictable nature, due to which a stand-alone PV or wind system is going to be less reliable and the power generated will be having strong fluctuations. But, the unique feature of wind and PV sources is their complementary nature, since wind is sufficiently available during the night times and cloudy conditions where as it is very insufficient during the sunny days [1].

A hybrid energy system can be made by combining both these sources, which is a more reliable and cost effective solution due the advantage of the complementary nature of these sources. Adding up the battery to store the excessive energy and to deliver it back when the power is in deficit makes a hybrid PV-wind-battery energy system.

As the number of sources increases, sizing of the various components of the system is necessary to utilize the resources to the full possible extent as well as to keep the system cost minimum while maintaining the reliability. Several authors have used single-objective optimization methods [2–6] and multi-objective optimization techniques [7–11] for solving the optimization problem. The objective in the single objective optimization is to minimize the cost while satisfying the system reliability constraint. But, in the multi-objective problem, the objectives include system cost, reliability. Some of the studies have considered pollutant emissions [11], and mismatch in energy. These objectives have been achieved by using iterative, graphical, probabilistic and analytical methods. The evolutionary algorithms, genetic algorithm (GA) [12–14], particle swarm optimization [15], levy flight (particle swarm optimization (PSO)) [16] and artificial bee swarm algorithm [17] are also widely used for the optimization problems. Along with the improved fruit fly algorithm [18], the harmony search [19,20] in combination with simulated annealing and chaotic search has been used for optimal sizing applications. Socio-demographic factors

Received Jul. 5, 2016; accepted Oct. 8, 2016; online Jul. 24, 2017

Aeidapu MAHESH (✉), Kanwarjit Singh SANDHU (✉)
Department of Electrical Engineering, National Institute of Technology,
Kurukshetra 136119, India
E-mail: mahesh.aeidapu@gmail.com; kjssandhu@rediffmail.com

such as different load curves to different type of customers have been used [21,22] in which two indices such as human development index and job creation index are considered for optimization. The energy storage has been sized in a PV/wind hybrid system for fluctuation minimization [23]. Along with PV, wind and battery tidal energy have also been considered for optimization [24].

The other problem with the sources such as PV and wind is the unpredictable nature, due to which the power output of the hybrid system contains strong fluctuations. To solve this issue, a few researchers [25–31] have used various control strategies for a hybrid system. A control strategy for switching of the different battery sections has been proposed [25,26] for a PV/wind/battery system. Fuzzy logic [29,32] has also been used to regulate the output power fluctuations for a PV/diesel system integrated to the grid. A low pass filter has been used to reduce the power fluctuations [28,33]. This method also has the disadvantage of setting of several time constants and inability to filter the fluctuations effectively.

The methods [25–30] used by the researchers are able to yield good results, but an optimal sizing strategy which includes the following constraints, such as less fluctuations in the power injected to the grid, full utilization of complementary characteristics would be a much better solution in terms of cost effectiveness and system reliability.

In view of the above issues, an optimal sizing strategy for a grid connected PV/wind/battery system has been proposed in this paper. The constraints used for optimization are loss of power supply probability, full utilization of complementary characteristics, fluctuations in the power injected into the grid, and the battery state of charge (SOC). The main objective function is minimizing the leveled cost of energy, while satisfying the above constraints. To solve multi-objective optimization problems effectively, GA has been used for optimization and a simple and easy to implement energy filter algorithm has been proposed to regulate the power injected into the grid.

2 System description and modeling

A DC-bus architecture for the hybrid system has been adopted as shown in Fig. 1, due to its simple interconnection and control over the AC-bus or hybrid-bus architecture. All the respective sources are converted to the common DC voltage and fed to the bus for supplying the load and to the grid where they are converted to AC by using an inverter and a step-up transformer. The DC/DC converter and the AC/DC converters connected to the PV and wind system respectively will perform the maximum power point tracking while the battery is the simple representation of multiple batteries connected in series and parallel.

2.1 PV system modeling

The output power and the efficiency of a PV cell are given by Eqs. (1) and (2).

$$P_{pv} = AG\eta_{pv}, \quad (1)$$

$$\eta_{pv} = \eta_{STC}[1 + \alpha(T_c - 25)], \quad (2)$$

where P_{pv} is the output power, A is the surface area of the panel in m^2 , G is the solar irradiation in (W/m^2) , η_{pv} and η_{STC} are the efficiencies under normal and standard test conditions, α is the temperature coefficient in $(\%/^{\circ}C)$, and T_c is the cell temperature in degrees.

By combining Eqs. (1) and (2), the output power can be expressed as in Ref. [23],

$$P_{pv} = P_{STC}f_{dr} \left\{ \frac{G}{1000}[1 + \alpha(T_c - 25)] \right\}, \quad (3)$$

where the factor f_{dr} indicates the de-rating factor, which will take the effect of dust and icing on the panels. The cell temperature can be calculated using the equation, given by

$$T_c = T_a + \left[\frac{NOCT - 20}{800} \right] G, \quad (4)$$

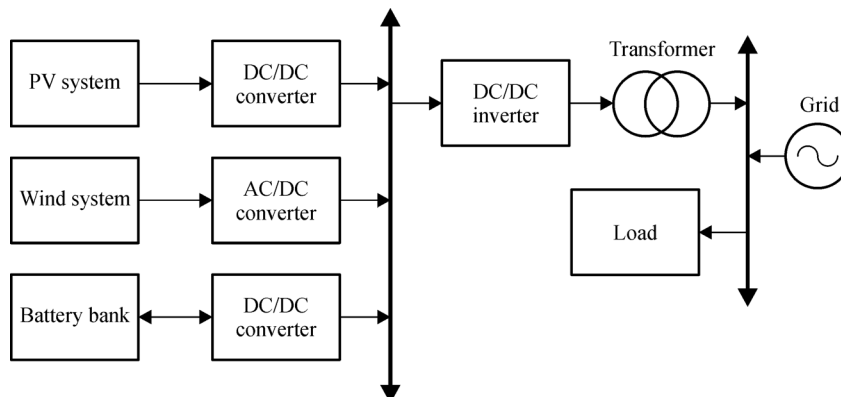


Fig. 1 Block diagram representation of hybrid PV-wind-battery system

where T_a is the ambient temperature in °C and NOCT is the nominal operational temperature of cell, which is generally 45°C to 47°C.

2.2 Wind system modeling

A typical wind turbine power curve as shown in Fig. 2 has been used to model the wind system. The turbine starts producing the power at a wind speed of 3 m/s. The rated power wind speed is 11 m/s and the wind turbine cuts off when the wind speed exceeds 25 m/s.

The wind characteristic equation is given by [33]

$$P_{WT} = \begin{cases} 0 & v_w < V_{ci} \text{ or } v_w > V_{co}, \\ P_{wt_r} \frac{v_w - V_{ci}}{v_r - V_{ci}} & V_{ci} < v_w < v_r, \\ P_{wt_r} & v_r < v_w < V_{co}, \end{cases} \quad (5)$$

where P_{wt_r} is the power at the rated wind speed v_r , v_w is the wind speed at that instant; V_{ci} and V_{co} are the cut-in and cut-off wind speed of the wind turbine.

2.3 Battery modeling

The battery has been modeled using the SOC model, in which the SOC at the instant $t + 1$ is estimated based on the SOC at the instant t , given by [2]

$$SOC(t + 1) = SOC(t) \cdot \left(1 - \frac{\sigma \Delta t}{24}\right) + \left(\frac{I_{bat}(t) \cdot \Delta t \cdot \eta_{bat}}{C_{bat}}\right), \quad (6)$$

where σ is the self discharge rate, I_{bat} is the charge or discharge current and η_{bat} is the charge/discharge efficiency of the battery, Δt is the time interval, and C_{bat} is the battery capacity in Ah.

The battery floating charge is calculated by the fitting of curve for the voltage polynomial in terms of SOC, which is given by

$$V_{bat} = A(SOC)^3 + B(SOC)^2 + C(SOC) + D, \quad (7)$$

where A , B , C , and D are functions of battery current and can be found by fitting the equations into the battery performance data provided by the manufacturer, using least squares method.

3 Economic modeling

The total annual cost of the system is given by

$$C_{A_total} = C_{inv} + C_{o\&m} + C_{gp} - C_{gs} + C_r + C_{pc}, \quad (8)$$

where C_{inv} is the investment cost which includes the cost of the various equipment in the system like PV panels, wind turbines, battery banks, inverters, and the other necessary equipment. $C_{o\&m}$ is the operation and maintenance cost, C_{gs} and C_{gp} are the cost of the power supplied to the grid and the power drawn from the grid respectively, C_r is the replacement cost which is generally taken into account when the life time of a particular component is less than the life time of the project, and C_{pc} is given by the penalty cost.

In the grid connected operation, the penalty cost will be levied once the system reliability goes below a specified limit given by β_L . Besides, the fluctuation in the power injected into the grid can also cause the penalty if it exceeds the limit β_g . So, the penalty cost is given by

$$C_{pc} = C_{pc1} (LPSP - \beta_L) \sum_{i=1}^N P_L(t_i) + C_{pc2} \frac{D_{gs} - \beta_g}{\beta_g} \times 100, \quad (9)$$

if $(LPSP > \beta_L)$ and $(D_{gs} > \beta_g)$,

where C_{pc1} is the penalty cost for the shortage of supply (\$/kWh) and C_{pc2} is the cost for fluctuation in the supply (\$/%).

The levelized cost of energy (LCE) is expressed by the total cost of the hybrid system divided by the total energy

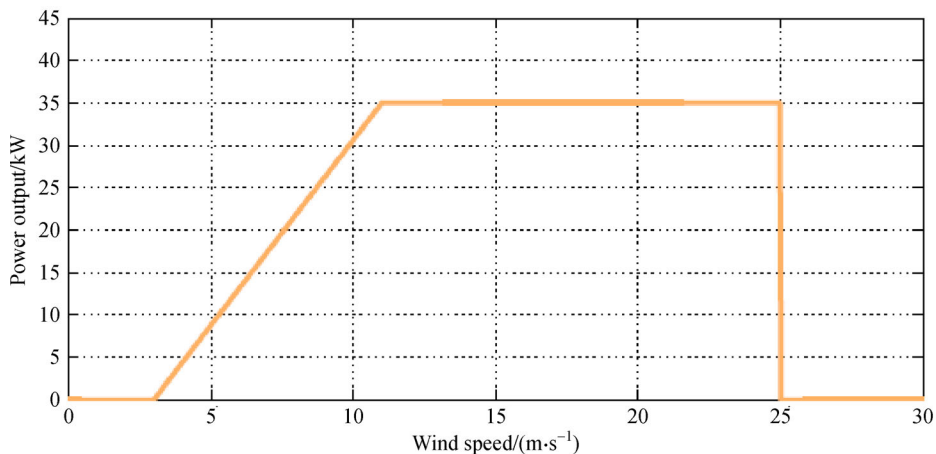


Fig. 2 Wind turbine characteristics

generated by the system, given by

$$\text{LCE} = \frac{C_{A_total}}{E_{total}}, \quad (10)$$

where E_{total} gives the total energy supplied by all three sources together. This LCE can be used to optimize the system economically.

4 Energy balance

The energy balance in grid connected mode is achieved as follows. In case the load demand is more than the supply, the rest of the power is to be purchased from the grid.

$$P_L(t) = P_{pv}(t) + P_{wt}(t) + P_{bs_dch}(t) + P_{gp}(t), \quad (11)$$

where $P_{gp}(t)$ is the power purchased from the grid. Similarly, when the power is in surplus, the excessive energy after charging the batteries will be supplied to the grid, given by

$$P_{gs}(t) = P_{pv}(t) + P_{wt}(t) - P_{bs_ch}(t) - P_L(t), \quad (12)$$

where $P_{gs}(t)$ is the power supplied to the grid at an instant of time.

5 Constraints

The reliability of the system is modeled in terms of loss of power supply probability (LPSP) in this paper. LPSP can be defined as the amount of the load that the system is not able to satisfy divided by the total load during the study period. It is given by

$$\text{LPSP} = \frac{\sum_{i=1}^N \frac{P_L(t_i) - P_{supplied}(t_i)}{\sum_{i=1}^N P_L(t_i)}, \quad (13)$$

where $P_{supplied}(t_i)$ is the total sum of energy supplied by the system at time t_i , and N is the total number of hours. In this paper, N is taken as 8760, the total number of hours in a year. So, the constraint for the reliability is given by

$$\text{LPSP} \leq \beta_L, \quad (14)$$

where β_L is the tolerance limit of the reliability of the system.

The fluctuations of power injected into the grid are defined by the Median absolute deviation (MAD) and fluctuation rate D_{gs} , given by

$$\text{MAD} = \text{median}_i(|P_{gs}(i) - \text{median}_j(P_{gs}(j))|), \quad (15)$$

$$D_{gs} = \frac{P_{gs_max} - P_{gs_min}}{\Delta t}, \quad (16)$$

where P_{gs_min} and P_{gs_max} are the minimum and the maximum power supplied to the grid in the time interval Δt . MAD gives the robust measure of variability of the univariate data. These two parameters, D_{gs} and MAD, can give the short and long term fluctuations of the power injected into the grid.

As the fluctuations, if they are exceeding a certain limit β_g , can lead to the penalty cost according to Eq.(9), the constraint for power fluctuations is given by

$$D_{gs} \leq \beta_g. \quad (17)$$

According to Ref. [33], the allowable maximum fluctuation in the power injected to the grid is 33% of the installed capacity within 10 minutes.

Full utilization of the complementary characteristics will ensure that the more power is supplied by the PV and wind system and the requirement of the high battery bank capacity is reduced. For that purpose, a factor has been used in this paper called complementary factor F_{compl} , given by

$$F_{compl} = \frac{1}{\bar{P}_L} \left\{ \sqrt{\frac{1}{N} \sum_{i=1}^N (P_{pv}(t_i) + P_{wt}(t_i) - P_L(t_i))^2} \right\}, \quad (18)$$

where \bar{P}_L is the average load. This factor gives the information about the closeness of the generated power to the load. A smaller value of F_{compl} gives a better complimentary characteristics between PV and wind sources.

$$F_{compl} \leq \beta_F. \quad (19)$$

As far as the batteries are concerned, in this method, the battery SOC is maintained within the minimum (SOC_{min}) and maximum (SOC_{max}) limits to ensure that the battery is neither completely discharged nor fully charged at any point of time. This will improve the battery life time. The constraint for this is given by

$$\text{SOC}_{min} \leq \text{SOC} \leq \text{SOC}_{max}. \quad (20)$$

Along with the SOC constraint, the charge (P_{bs_ch}) and discharge power (P_{bs_dch}) at any point of time are to be kept within the maximum charge and discharge power limits to regulate the flow of charge to the battery. Besides, the charge (P_{bs_ch}) and discharge currents (I_{bs_dch}) are to be maintained within the limits.

6 Optimization strategy

In the multi-objective problem solution, to achieve all the objectives, one of the objectives is chosen as the final objective function, the rest of the objectives are treated as constraints and the final objective function is then solved

as a single objective problem. So, the main objective function is the minimization of the LCE, given by

$$\text{Min}f = \min(\text{LCE}). \quad (21)$$

After satisfying the constraints given by Eqs. (14), (17) and (20), the combination with the lowest LCE will be the final optimal solution for the problem.

6.1 Genetic algorithm

GA is a population based stochastic optimization tool, which has an ability to solve the multi-objective problems. In this algorithm, initially, a set of randomly generated population from the solution space is used to generate a set of initial solutions to the problem. The fitness function is evaluated individually for each solution and the solutions are ranked according to their fitness value. Then, this population is going to be evolved through different operations called crossover, reproduction, and mutation to find out the final optimal solution in an iterative manner. Most conventional algorithms suffer a great deal in solving the non-convex optimization problems, because they have more chances to get trapped in the local-optima. But, GA can find the global optimum solution to the non-convex, non-linear and non-smooth optimization problems because of its ability to search for the solution in the entire solution space.

6.2 Proposed optimization strategy without energy filter

The flowchart of the proposed optimization strategy using GA is represented in Fig. 3. By using the randomly generated initial population, initial solutions and their respective parameters for the optimization given by Eqs. (13), (15), (16) and (18) will be evaluated. After that, the constraints given by Eqs. (14), (17) and (20) are checked and the final fitness function will be evaluated. Then, the process of crossover and mutation takes place, and this entire process will be repeated until the final optimum solution is reached. The parameters used for the GA are presented in Table 1.

Table 1 Parameters used for GA

Parameter	Population size	Maximum generation	Crossover probability	Mutation probability	Elitism probability
Value	40	50	0.9	0.005	0.1

6.3 Proposed optimization strategy with energy filter

As can be seen from Fig. 3, the optimization strategy without filter can take care of reliability issues, but it does not include the effect of fluctuations of the power injected into the grid. The power which is left after supplying the charging power to the batteries is directly fed into the grid.

So, this can cause large fluctuations to the power injected into the grid and can cause an additional penalty cost according to Eq. (9).

To solve this problem, an energy filter has been proposed [33], which is a second order low-pass filter modeled using the equation given by

$$f(s) = \frac{\omega_n^2}{S^2 + (\omega_n/Q)s + \omega_n^2}, \quad (22)$$

where Q is the quality factor and ω_n is the cut-off frequency.

The energy filter is an algorithm, which separates the high frequency and high frequency components from the power injected into the grid. Unlike the previous method which directly injects power into the grid, the power here is supplied to the filter and the low frequency component is supplied to the grid while the high frequency component is supplied to the batteries.

The discrete time domain representation of the equation is given by Eq. (22) with a sampling period T_s . The following equation gives the separation of low frequency component from the signal, given by

$$\frac{P_{gs_LF}}{P_{gs}} = \frac{\omega_n^2}{((1-z-1)/T_s)^2 + \frac{\omega_n}{Q} \frac{1-z-1}{T_s} + \omega_n^2}. \quad (23)$$

The high frequency component, which is fed to the battery, is given by

$$P_{gs_HF} = P_{gs} - P_{gs_LF}. \quad (24)$$

The optimization strategy for the case of energy filter is also just like the case without filter, but by including the constraint for the power fluctuations injected into the grid, it is given by Eq. (17).

The fluctuations of the power injected into the grid are reduced considerably by using this energy filter. But, it has some disadvantages, which would reduce its applicability for the hybrid systems. Here, the sampling time T_s plays an important role in the power supplied to the grid as well as the power supplied to the batteries. If it is not chosen properly, it can cause either more fluctuations or less reliability to the system. In addition, this filter does not guarantee that the value of P_{gs_LF} is always less than the current P_{gs} value, which may result in the discharge of batteries even when there is excess of power available. This will cause the batteries to charge/discharge more and will surely affect the life time of the batteries.

In order to avoid these problems caused by the energy filter, a novel energy filtering algorithm has been proposed in this paper. The flowchart of the algorithm is shown in Fig. 4. In this method, the fluctuation in the power injected into the grid is reduced to a level which is acceptable according to the constraint (17). For that, first the deviation is calculated between the present and the previous value

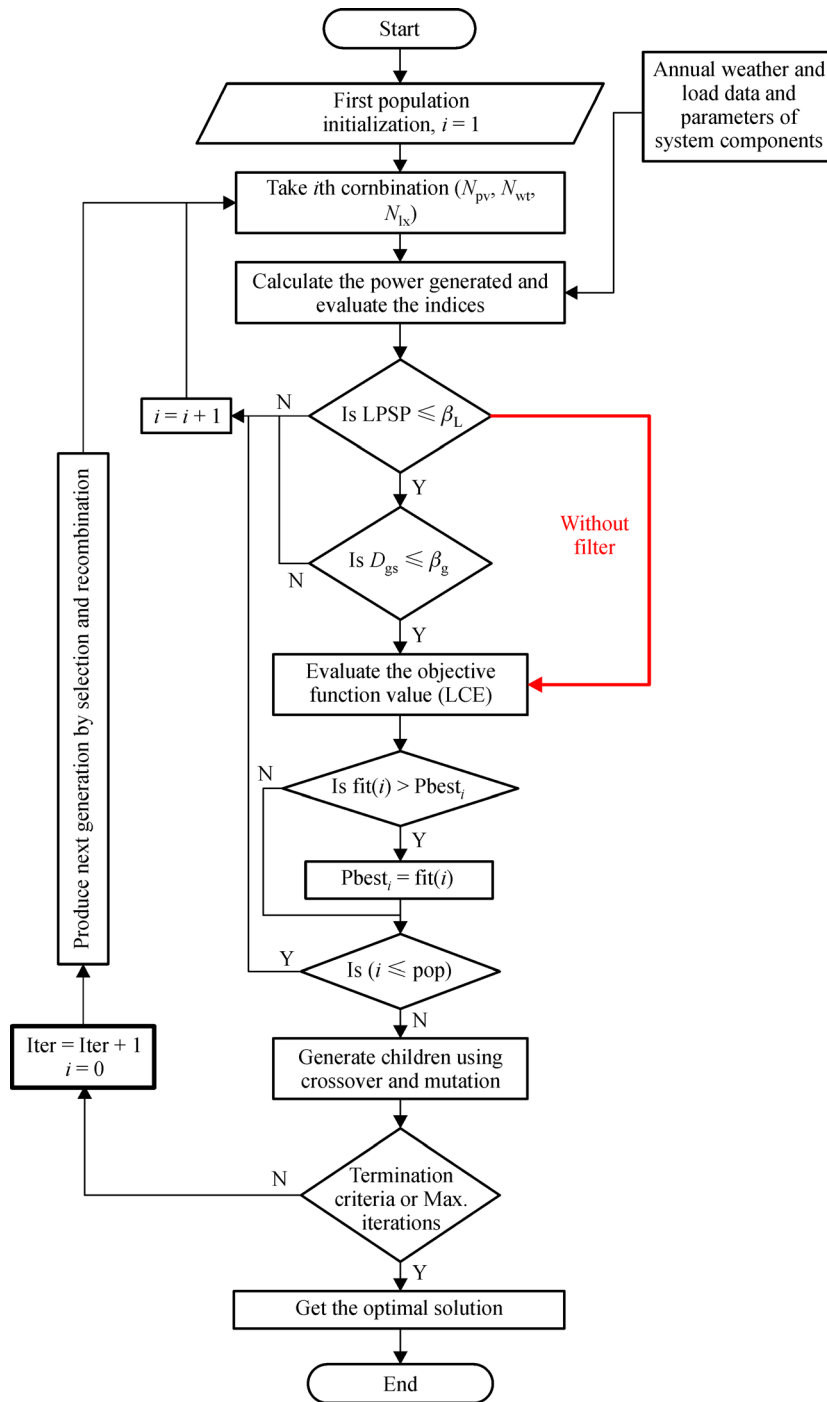


Fig. 3 Proposed optimal sizing strategy

using

$$Dev = P_{gs}(i) - P_{gs}(i-1). \quad (25)$$

Then, based on the value of Eq. (25), the effective value of the power injected into the grid P_{gsef} can be calculated as

$$P_{gsef}(i) = \begin{cases} P_{gs}(i) & \text{if } (0 \leq Dev < \beta_g), \\ P_{gs}(i-1) + 0.95\beta_g & \text{if } (Dev \geq \beta_g), \\ P_{gs}(i) & \text{if } (Dev < 0). \end{cases} \quad (26)$$

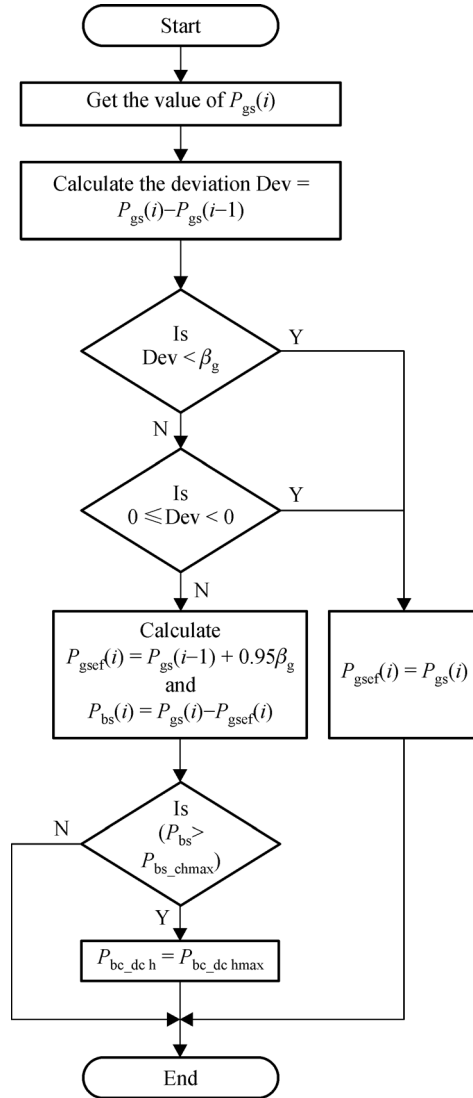


Fig. 4 Proposed energy filter algorithm

The power supplied to the batteries is the difference between P_{gs} and P_{gsef} , given by

$$P_{bs} = P_{gs} - P_{gsef}. \quad (27)$$

In this algorithm, only the fluctuations caused by the rise in power, i.e., in the case the Dev is positive, have been taken care of. If the negative deviation cases also have been taken into account, to reduce the fluctuations, there must be extra power supplied to the grid, which has to come from the batteries. This will cause the batteries to discharge even more, thereby reducing the life time of batteries. Here, a factor of 0.95 is chosen such that the fluctuations would always stay under the acceptable limit β_g .

7 Case study and results

To show the effectiveness of the proposed methodology, a

case study has been presented in this section. The various meteorological data patterns employed are depicted in Fig. 5.

Figure 5(a) shows the hourly irradiation pattern while Fig. 5(b) shows the monthly average temperature. The wind speed pattern is demonstrated in Fig. 5(c). It can be seen that the average wind speed of the pattern is 5.33 m/s and the maximum wind speed is 25.257 m/s. The hourly load pattern is presented in Fig. 5(d). It can be observed that the average load is 78 kW and the maximum load is about 264 kW with a load factor of 0.2953.

The specifications and the various costs of the PV panel and wind turbine and battery bank used are listed in Table 2. The variables used for calculation of PV output α_t is taken as -0.48 and f_{dr} is taken as 85%. As it is assumed that the PV is operating under the maximum power point (MPP) condition, the factor f_{MPP} is taken as 1. The maximum charge on the battery Q_{max} is taken as 720 Ah and the parameters k and c are taken as 0.34 and 0.98 respectively.

7.1 Analysis of simulation results without energy filter

The results of the proposed optimization strategy are tabulated in Table 3 without considering any energy filter. Moreover, Fig. 6 shows the annual pattern for the total energy generated by the system. The power injected into the grid is displayed in Fig. 7. From the results, it can be seen that the strategy employed is yielding good results in terms of reliability, but it is unable to meet the desired fluctuation criteria.

7.2 Analysis of simulation results with energy filter

The results of optimization after applying the energy filter according to Eq. (22) are shown in Table 4. Figure 8 illustrates the annual pattern of the power injected into the grid after employing an energy filter. The power supplied to the battery is shown in Fig. 9.

From Table 4, it can be clearly seen that the strategy after employing the energy filter has shown a considerable improvement in terms of fluctuations of the power injected into the grid as the value of D_{gs} is less than the value of β_g and the reliability criteria is met. But, the required battery has been increased enormously and as a result, the cost per unit of electricity has also been increased to 0.58.

The reason for this can be explained from Figs. 8 and 9. As the difference between the power before and after compensation is the power supplied to the battery, in this case, from Fig. 9 it can be clearly seen that many times the power after compensation is more than the power before compensation. This extra power needs to be supplied from the batteries which cause them to discharge even when the power is in surplus. Besides, it can be seen that when the difference is positive, it is quite small and not enough for the batteries to get adequate charge. This can be seen from

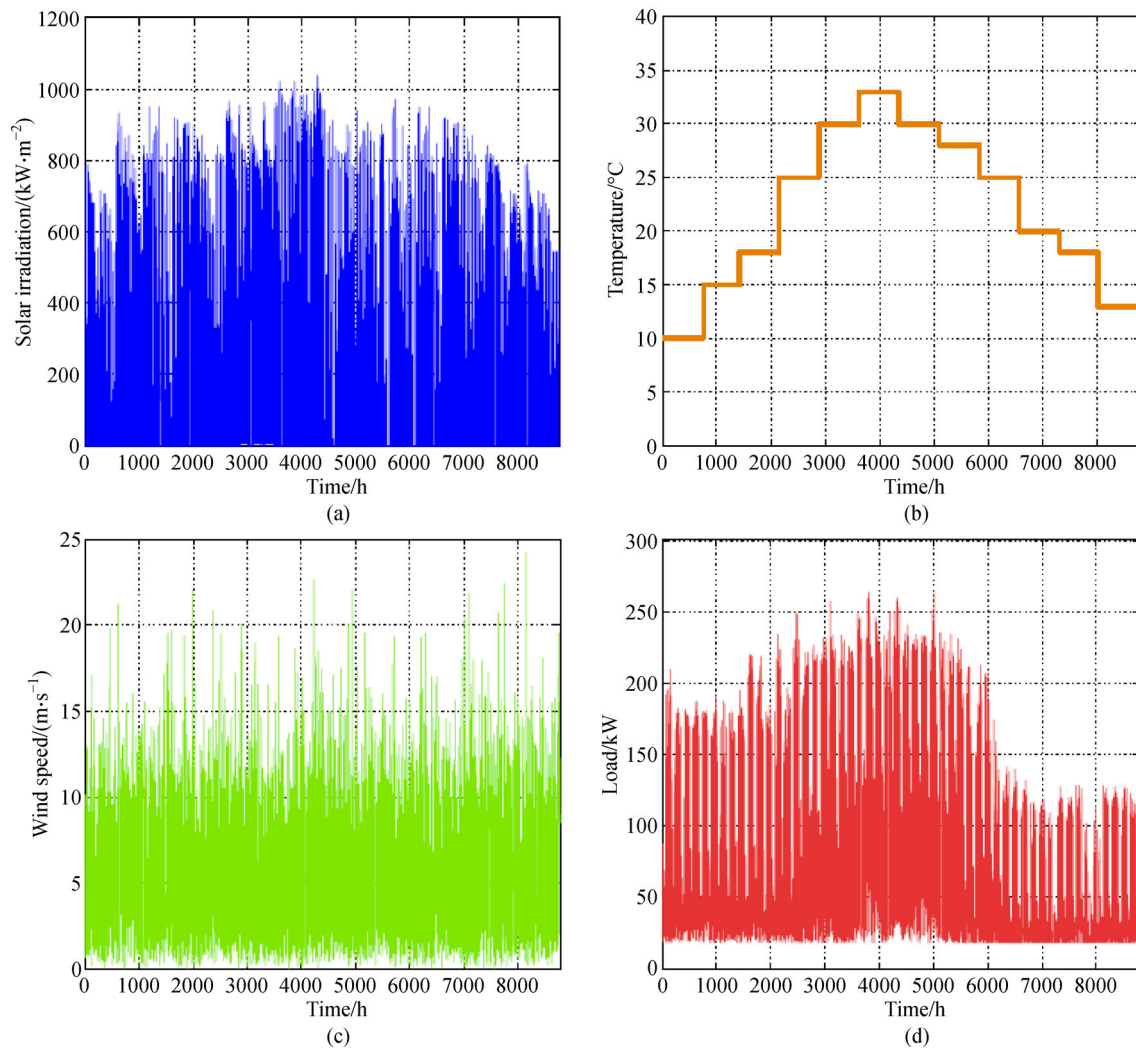


Fig. 5 Meteorological data and load patterns

(a) Hourly irradiation pattern; (b) monthly average temperature; (c) hourly wind speed pattern; (d) hourly load pattern

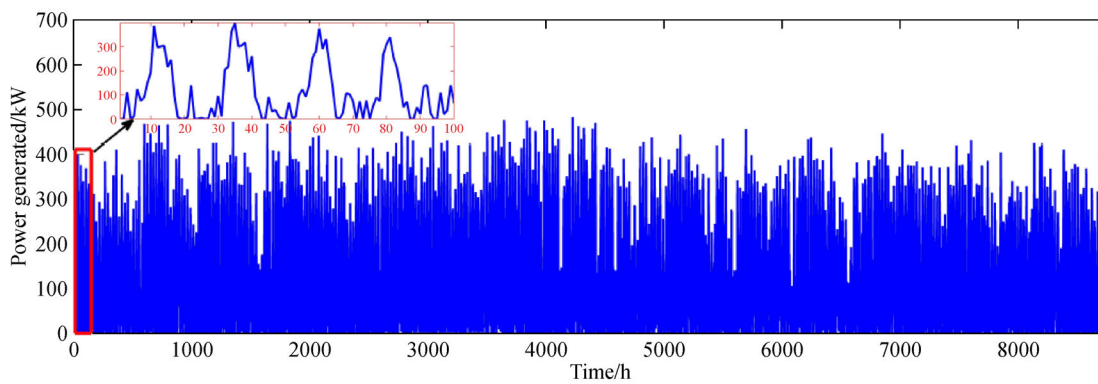


Fig. 6 Power generated by the hybrid system

Table 2 Parameters of system components

	Parameter	Value
PV panel: SANYO HIT Power 200	Maximum power/W	200
	OC voltage /V	68.7
	SC current/A	3.83
	Voltage at MPP/V	55.8
	Current at MPP/A	3.59
	Efficiency at STC	17.2
	Slope (fixed slope)/(°)	40.98
	Cost per panel (C_{pv})/\$	420
	O & M cost ($C_{pvo\&m}$)/(\$·kW ⁻¹)	15
	Wind turbine: PGE 35 kW	Rated power/kW
Cut-in wind speed/(m·s ⁻¹)		3
Cut-out wind speed/(m·s ⁻¹)		25
Hub height/m		24
Rated wind speed/(m·s ⁻¹)		11
Rotor diameter/m		19.2
Blade length/m		9
Cost per turbine (C_{wt})/\$		25000
O & M cost ($C_{wto\&m}$)/(\$·kW ⁻¹)		30
Battery: Hoppecke 6OPzS 600		Rated capacity/Ah
	Rated voltage/V	2
	Round trip efficiency/%	85
	Max. Ch./disch. rate/(A·Ah ⁻¹)	0.5
	Max. ch/dis. current/A	100, 75
	A self-discharge rate/%	1
	Cost per battery (C_{bs})/\$	150
	O & M cost ($C_{bso\&m}$)/(\$·kAh ⁻¹)	20

Table 3 Results of optimal sizing without energy filter

N_{pv}	N_{wt}	N_{bs}	LPSP	MAD/kW	F_{compli}	β_g /kW	D_{gs} /kW	LCE
2107	4	1502	0.05	111.64	2.5	46.2	98.6	0.4223

Table 4 Results of optimal sizing with energy filter

N_{pv}	N_{wt}	N_{bs}	LPSP	MAD(kW)	F_{compli}	β_g /kW	D_{gs} /kW	LCE
1843	11	2733	0.05	158.16	2.3	121.638	115.53	0.5856

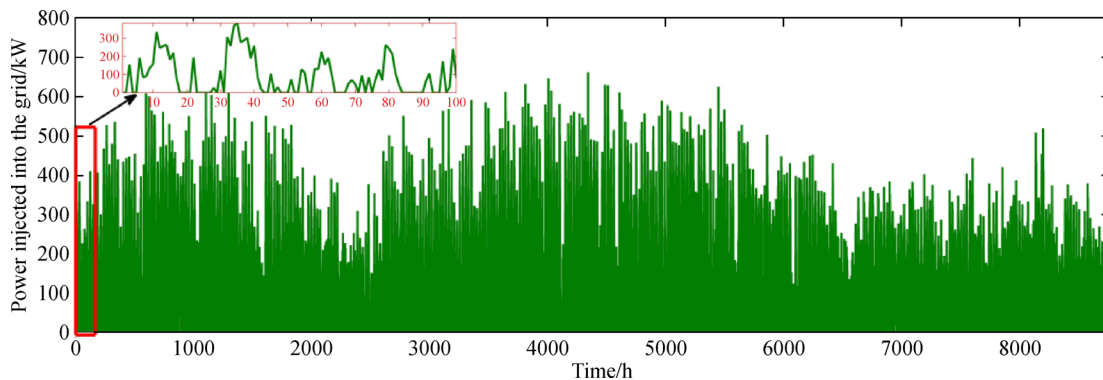
Fig. 9. If the value of P_{bs} is positive, the battery is discharging and if it is negative, it is charging. It can be seen that the duration of time that the battery discharges is more than the duration of time it is charging. This causes the batteries to discharge more, which is the reason for the poor reliability and increased cost due to the requirement of more batteries.

7.3 Analysis of simulation results with proposed energy filter algorithm

The results of the optimization after considering the proposed energy filter algorithm are given in Table 5. Figure 10 shows the annual pattern of the power injected into the grid both with and without filter. Figure 11 exhibits the plot of objective function value with the number of iterations. From Fig. 11, it can be seen that the objective function has been minimized very quickly within 10 iterations.

From Table 5, it can be seen that the optimizing strategy employing the proposed energy filter is able to yield better results when compared to both of the previous cases as it meets both the reliability and the fluctuation criteria. Besides, the full utilization of complementary characteristics is also achieved as the factor F_{compli} is 0.402, which is a very low value.

From Fig. 10 it can be seen that, unlike the previous case, the actual power supplied into the grid is always less than the power injected in the case without filter, which indicates that the batteries are always going to charge whenever there is excess of power. Figure 12 shows that in all times the SOC of the battery is within the limits. This justifies the fact that the battery is having a healthy charge all the time, which implies that the battery lifetime will be longer. Figure 13 gives the probability for different

**Fig. 7** Power supplied to the grid without filter

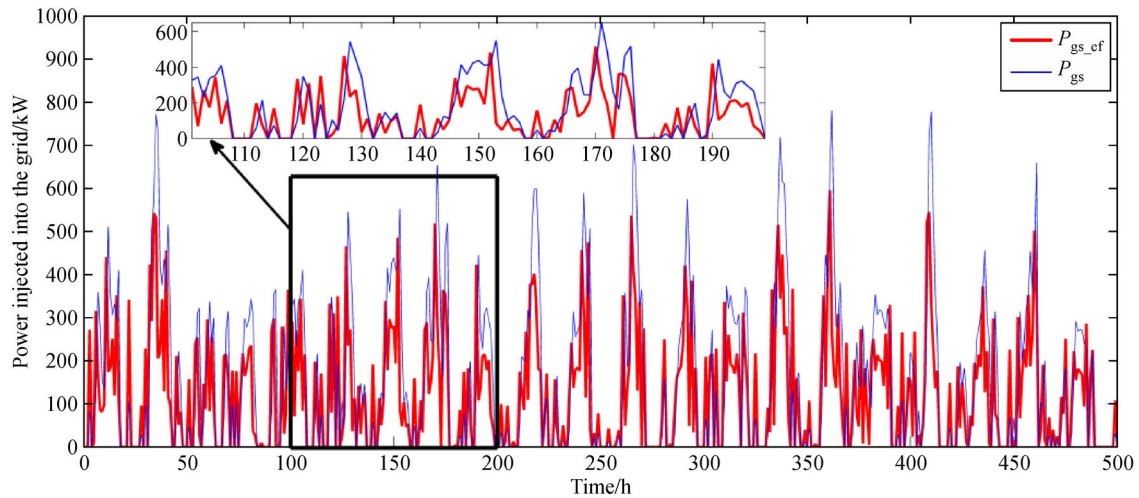


Fig. 8 Comparison of power injected into the grid

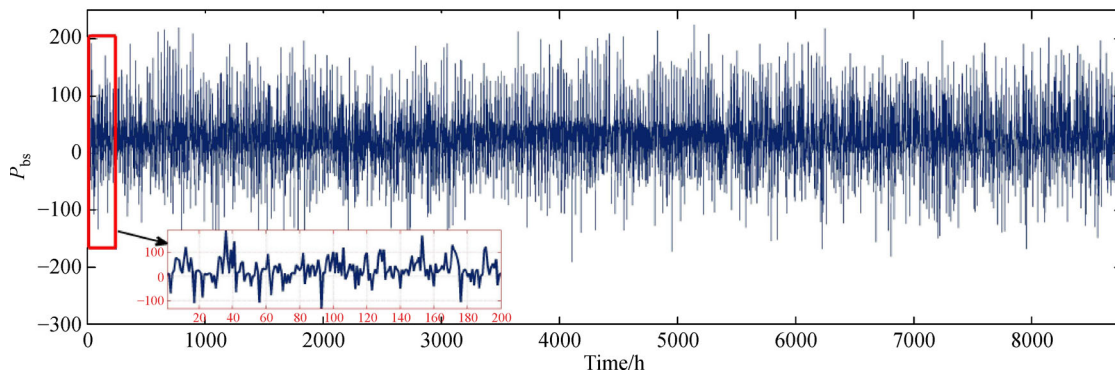


Fig. 9 Battery power with energy filter

Table 5 Results of optimal sizing with proposed energy filter

N_{pv}	N_{wt}	N_{bs}	LPSP	MAD/kW	F_{compli}	β_g/kW	D_{gs}/kW	LCE
1902	11	1056	0.049	86.37	2.1	125.532	95.79	0.4024

fluctuation rate ranges. From Fig. 13, it can be seen that, with the proposed filter, the probability of getting low fluctuations has been considerably increased when compared to the system without filter. In addition, the higher

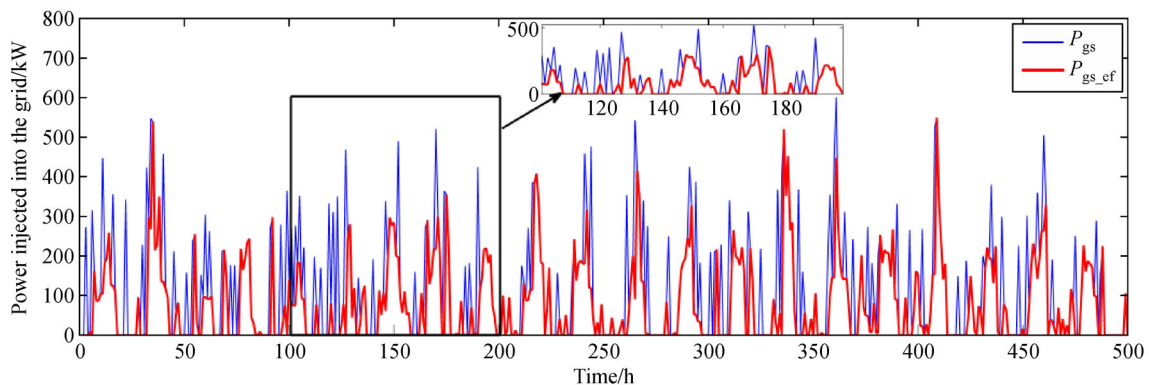


Fig. 10 Power injected into the grid with proposed energy filter

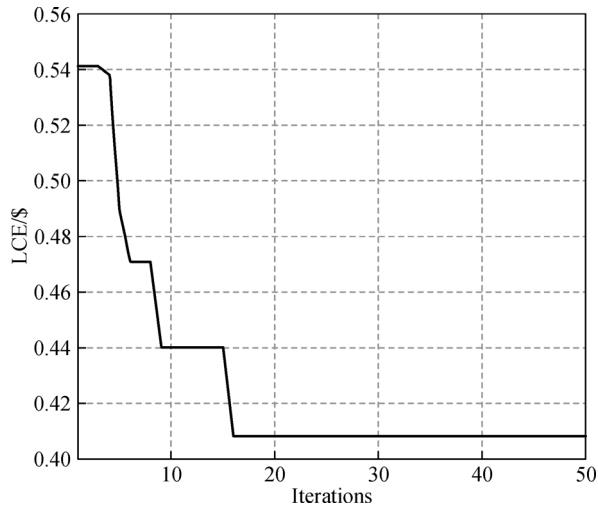


Fig. 11 No. of iterations versus cost function plot

fluctuations are also reduced to a very small level, which implies that the proposed strategy effectively eliminates the high fluctuations in the power injected into the grid.

Table 6 is a comparison of the three strategies discussed in this paper. It can be seen that the total cost for the entire system is low in the third case. And there is a penalty cost imposed in the case without filter, because of the violation of the fluctuation criteria, but the penalty cost is absent in the case of proposed energy filter because it meets all the required criteria. Therefore, from these results it can be justified that the proposed novel energy filter algorithm and the optimization strategy are able to achieve the entire desired criterion while maintaining the minimum cost.

8 Conclusions

In this paper, an improved optimal sizing strategy based on

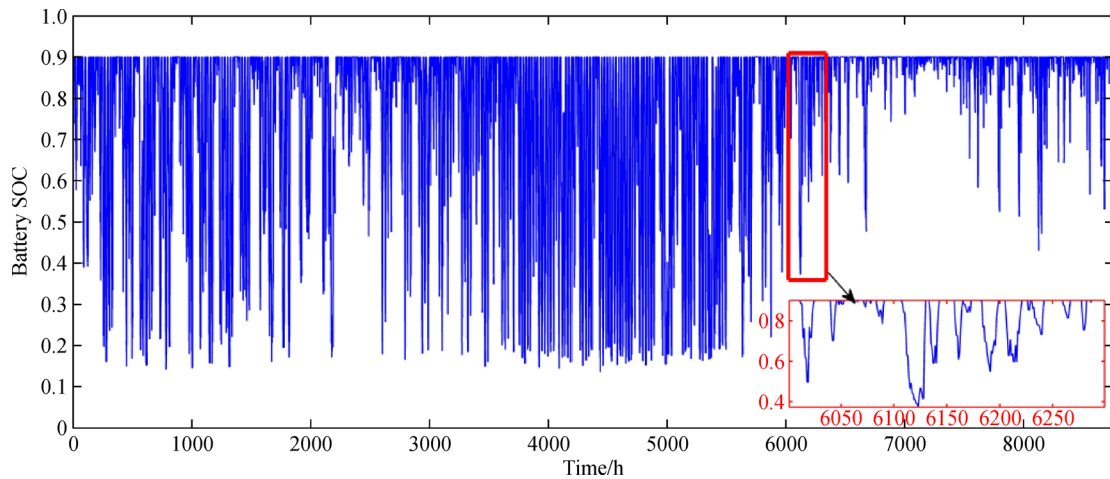


Fig. 12 Battery state of charge

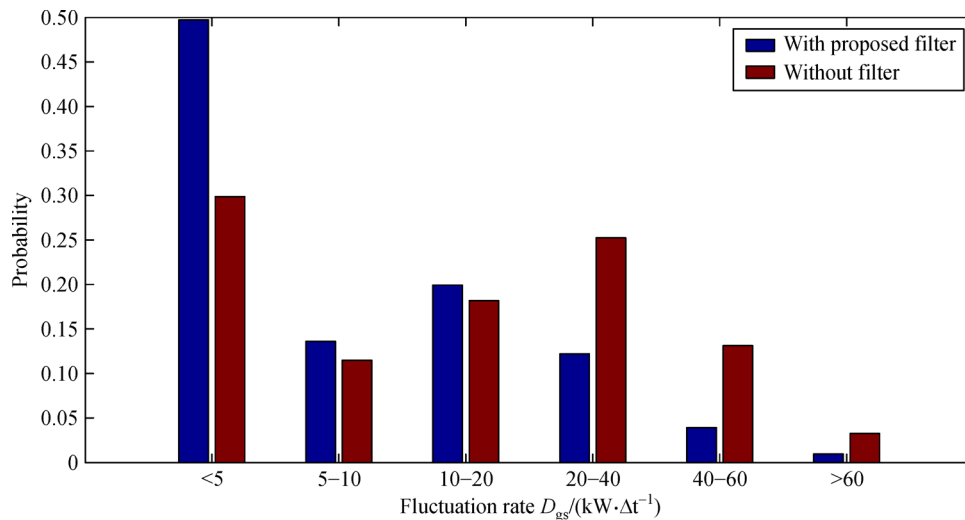


Fig. 13 Probability of fluctuation rate

Table 6 Comparison of three strategies

Parameter	Without filter	With energy filter	With proposed filter
$C_A(\times 10^5)/\$$	2.879	3.99	2.74
LCE/\\$	0.4223	0.5856	0.4024
$C_{pc}(\times 10^6)/\$$	5.6717	0	0
$D_{gs}(kW/\Delta t)$	98.6	115.53	95.79
$\beta_g(kW/\Delta t)$	56.1	69.3	115.5
F_{compl}	2.5	2.3	2.1
LPSP	0.05	0.05	0.049
MAD	111.64	158.16	86.37
$N_{gs}(\times 10^8)$	9.233	15.05	7.20
$N_{gp}(\times 10^7)$	3.33	2.461	3.352

GA has been proposed with an energy filter algorithm. The modeling of PV, wind and battery systems along with the economic model have been presented. The improved optimization model which takes fluctuations of power injected into the grid, system reliability and complementary characteristics into consideration has been developed and simulated using the GA. The energy filter algorithm has been developed and implemented for optimal sizing of the various system components. The effectiveness of the proposed methodology is demonstrated with the help of a case study as presented and discussed. The results for the three different cases, without filter, with already existing filter and with the proposed filter have been compared. From the results it can be concluded that the proposed method with the developed energy filter algorithm gives the cost-effective combination of the system components, while satisfying all the required constraints.

References

1. Mahesh A, Sandhu K S. Hybrid wind/photovoltaic energy system developments: critical review and findings. *Renewable & Sustainable Energy Reviews*, 2015, 52: 1135–1147
2. Yang H X, Lu L, Zhou W. A novel optimization sizing model for hybrid solar-wind power generation system. *Solar Energy*, 2007, 81(1): 76–84
3. Ekren O, Ekren B Y. Size optimization of a PV/wind hybrid energy conversion system with battery storage using simulated annealing. *Applied Energy*, 2010, 87(2): 592–598
4. Kaabeche A, Belhamel M, Ibtouen R. Sizing optimization of grid-independent hybrid photovoltaic/wind power generation system. *Energy*, 2011, 36(2): 1214–1222
5. Kellogg W D, Nehrir M H, Venkataramanan G, Gerez V. Generation unit sizing and cost analysis for stand-alone wind, photovoltaic, and hybrid wind/PV systems. *IEEE Transactions on Energy Conversion*, 1998, 13(1): 70–75
6. Markvart T. Sizing of hybrid photovoltaic-wind energy systems. *Solar Energy*, 1996, 57(4): 277–281
7. Dufo-López R, Bernal-Agustín J L. Multi-objective design of PV-wind-diesel-hydrogen-battery systems. *Renewable Energy*, 2008, 33(12): 2559–2572
8. Dufo-López R, Bernal-Agustín J L, Yusta-Loyo J M, Domínguez-Navarro J A, Ramírez-Rosado I J, Lujano J, Aso I. Multi-objective optimization minimizing cost and life cycle emissions of stand-alone PV-wind-diesel systems with batteries storage. *Applied Energy*, 2011, 88(11): 4033–4041
9. Yang H X, Zhou W, Lu L, Fang Z H. Optimal sizing method for stand-alone hybrid solar-wind system with LPSP technology by using genetic algorithm. *Solar Energy*, 2008, 82(4): 354–367
10. Diaf S, Diaf D, Belhamel M, Haddadi M, Louche A. A methodology for optimal sizing of autonomous hybrid PV/wind system. *Energy Policy*, 2007, 35(11): 5708–5718
11. Ren H B, Zhou W S, Nakagami K, Gao W J, Wu Q. Multi-objective optimization for the operation of distributed energy systems considering economic and environmental aspects. *Applied Energy*, 2010, 87(12): 3642–3651
12. Zhao B, Zhang X S, Li P, Wang K, Xue M D, Wang C S. Optimal sizing, operating strategy and operational experience of a stand-alone microgrid on Dongfushan Island. *Applied Energy*, 2014, 113: 1656–1666
13. Sheng W X, Liu K Y, Meng X L, Ye X S, Liu Y M. Research and practice on typical modes and optimal allocation method for PV-Wind-ES in microgrid. *Electric Power Systems Research*, 2015, 120: 242–255
14. Yazdanpanah Jahromi M A, Farahat S, Barakati S M. Optimal size and cost analysis of stand-alone hybrid wind/photovoltaic power-generation systems. *Civil Engineering and Environmental Systems*, 2014, 31(4): 283–303
15. Maleki A, Askarzadeh A. Artificial bee swarm optimization for optimum sizing of a standalone PV/WT/FC hybrid system considering LPSP concept. *Solar Energy*, 2014, 107: 227–235
16. Askarzadeh A. Solution for sizing a PV/diesel HPGS for isolated sites. *IET Renewable Power Generation*, 2017, 11(1): 143–151
17. Fetanat A, Khorasaninejad E. Size optimization for hybrid photovoltaic-wind energy system using ant colony optimization for continuous domains based integer programming. *Applied Soft Computing*, 2015, 31: 196–209
18. Zhao J Y, Yuan X F. Multi-objective optimization of stand-alone hybrid PV-wind-diesel-battery system using improved fruit fly optimization algorithm. *Soft Computing*, 2016, 20(7): 2841–2853
19. Ahmadi S, Abdi S. Application of the Hybrid Big Bang-Big Crunch algorithm for optimal sizing of a stand-alone hybrid PV/wind/battery system. *Solar Energy*, 2016, 134: 366–374
20. Maleki A, Pourfayaz F, Rosen M A. A novel framework for optimal design of hybrid renewable energy-based autonomous energy systems: a case study for Namin, Iran. *Energy*, 2016, 98: 168–180
21. Tito S R, Lie T T, Anderson T N. Optimal sizing of a wind-photovoltaic-battery hybrid renewable energy system considering socio-demographic factors. *Solar Energy*, 2016, 136: 525–532
22. Dufo-López R, Cristóbal-Monreal I R, Yusta J M. Optimisation of PV-wind-diesel-battery stand-alone systems to minimise cost and maximise human development index and job creation. *Renewable Energy*, 2016, 94: 280–293

23. Sandhu K S, Mahesh A. A new approach of sizing battery energy storage system for smoothing the power fluctuations of a PV/wind hybrid system. *International Journal of Energy Research*, 2016, 40 (9): 1221–1234
24. Askarzadeh A. Electrical power generation by an optimised autonomous PV/wind/tidal/battery system. *IET Renewable Power Generation*, 2017, 11(1): 152–164
25. Li X J, Hui D, Lai X K. Battery energy storage station (BESS)-based smoothing control of photovoltaic (PV) and wind power generation fluctuations. *IEEE Transactions on Sustainable Energy*, 2013, 4 (2):464–473
26. Li X J, Hui D, Wu L, Lai X K. Control strategy of battery state of charge for wind/battery hybrid power system. In:2010 IEEE International Symposium on Industrial Electronics (ISIE2010), Bari, Italy, 2010, 2723–2726
27. Ahmed N A, Miyatake M, Al-Othman A K. Power fluctuations suppression of stand-alone hybrid generation combining solar photovoltaic/wind turbine and fuel cell systems. *Energy Conversion and Management*, 2008, 49(10): 2711–2719
28. Kim S K, Jeon J H, Cho C H, Ahn J B, Kwon S H. Dynamic modeling and control of a grid-connected hybrid generation system with versatile power transfer. *IEEE Transactions on Industrial Electronics*, 2008, 55(4): 1677–1688
29. Datta M, Senjyu T, Yona A, Funabashi T, Kim C H. A coordinated control method for leveling PV output power fluctuations of PV/diesel hybrid systems connected to isolated power utility. *IEEE Transactions on Energy Conversion*, 2009, 24(1): 153–162
30. Omran W A, Kazerani M, Salama M M A. Investigation of methods for reduction of power fluctuations generated from large grid-connected photovoltaic systems. *IEEE Transactions on Energy Conversion*, 2011, 26(1): 318–327
31. Aissou S, Rekioua D, Mezzai N, Rekioua T, Bacha S. Modeling and control of hybrid photovoltaic wind power system with battery storage. *Energy Conversion and Management*, 2015, 89: 615–625
32. Datta M, Senjyu T, Yona A, Funabashi T. A fuzzy based method for leveling output power fluctuations of photovoltaic-diesel hybrid power system. *Renewable Energy*, 2011, 36(6): 1693–1703
33. Xu L, Ruan X B, Mao C X, Zhang B H, Luo Y. An improved optimal sizing method for wind-solar-battery hybrid power system. *IEEE Transactions on Sustainable Energy*, 2013, 4(3): 774–785